The first amidine based highly selective and colorimetric multi-ion sensor for Fe^{3+}, Fe^{2+} and Cu^{2+}

Jitendra Nandre[a], Samadhan Patil[a], Prashant Patil[a,b], Suban K. Sahoo[c], Carl Redshaw[d], Pramod Mahulikar[a]* and Umesh Patil[a*]

[a] School of Chemical Sciences, North Maharashtra University, Jalgaon, 425 001, INDIA, Email- jpnandre99@gmail.com (JP), samadhanp999@gmail.com (SP), mahulikarpp@rediffmail.com (PM), udpatil.nmu@gmail.com (UP), Phone-+91-257-2257432.

[b] S.S.V.P.S's L. K. Dr. P. R. Ghogrey Science College, Dhule-424 001, INDIA, patil.prashant86@rediffmail.com (PP).

[c] Department of Applied Chemistry, S. V. National Institute Technology, Surat-395 007, Gujrat, INDIA, Email- suban_sahoo@rediffmail.com (SKS).

[d] Department of Chemistry, University of Hull, Cottingham Road, Hull, HU6 7RX (UK).

Abstract

The amidine based chemosensor **AM-1** was synthesized by using 2-cyanopyridine and 4-bromoaniline. Its structure was established by using FT-IR and ^{1}H-NMR spectroscopy, mass spectrometry and by elemental analyses. Sensor **AM-1** exhibited high selectivity and sensitivity towards Fe^{3+}, Fe^{2+} and Cu^{2+} in the presence of other surveyed ions (such as Sr^{2+}, Cr^{3+}, Co^{2+}, Ni^{2+}, Zn^{2+}, Ag^{+}, Al^{3+}, Ba^{2+}, Ca^{2+}, Cd^{2+}, Hg^{2+}, K^{+}, Li^{+}, Mg^{2+}, Mn^{2+}, Na^{+} and Pb^{2+}) with a distinct naked-eye detectable colour change and a shift in the absorption band. However, the emission of **AM-1** was quenched selectively only in the presence of Fe^{3+}.

Key words: Amidine, Chemosensor, Chromogenic receptor, Multi metal ion sensor, DFT.

***Corresponding author:** Phone No.: +91-257-2257431, Fax No.: +91-257-2258403, E-mail: mahulikarpp@rediffmail.com (Dr Mahulikar) and udpatil.nmu@gmail.com (Dr Patil).

1. Introduction

Chemosensors are molecules of abiotic origin that reveal a significant change in electrical, electronic, magnetic or optical signals when interacting with a specific guest/s (ions/molecules) [1,2]. During the sensing process, information at the molecular level, such as the presence or absence of a certain guest in solution, is amplified to a macroscopic level; hence sensing might open the new door to the qualitative and quantitative determination of the guest. Additionally, among the various sensing methods, sensors based on a naked-eye response (colorimetric) have many advantages because of their ability to provide a simple, sensitive, selective, precise and economical method for the detection of a target analyte without the use of sophisticated instrumentation [3-6]. In colorimetric chemosensors, the spectral and visual colour changes are affected by the respective increase or decrease in the electron densities on the chromophoric moiety, which is effectively monitored by the recognition of a charged analyte, i.e., cation or anion.

The designed and synthesis of selective and sensitive chemosensors for detecting transition metal ions such as Fe^{3+}, Cu^{2+}, Zn^{2+}, Fe^{2+}, etc. has gained importance because of their involvement in a variety of fundamental biological and physiological processes in living systems including in human metabolic processes [7-10]. As important physiological relevant metal ions, both the Fe^{2+} and Fe^{3+} ions play an indispensable role in many biochemical processes at the cellular level. Numerous enzymes use Fe^{3+} as a catalyst for electron transfer, oxygen metabolism, and RNA and DNA synthesis [11,12]. However, both its deficiency (hypoferremia) and excess (hyperferremia) can induced a variety of diseases. The regulation of iron in the human body is a highly controlled process. The cellular toxicity caused by iron ions has been linked with several serious diseases, for example Alzheimer's, Huntington's and Parkinson's diseases [13,14]. Similarly, Cu^{2+} is a significant metal pollutant due to its widespread use [15]. Cu^{2+} is well known for its important role as a catalytic cofactor in a

variety of metallo-enzymes, including superoxide dismutase, cytochrome *c* oxidase and tyrosinase [16]. However, long-term exposure to high levels of Cu^{2+} has been reported to induce liver and kidney damage. Cu^{2+} also exhibits toxicity associated with neurodegenerative diseases such as Alzheimer's, Wilson's and prion disease [17-20]. Due to the significance of Cu^{2+}, Fe^{2+} and Fe^{3+} ions in physiological processes, a method for the rapid, sensitive and selective detection of such ions in food and/or pharmaceutical products, as well as biological samples such as blood, urine, etc. is of great significance. As a result, intense research effort has been focused on the development of sensitive and selective receptors for the qualitative and quantitative recognition of Cu^{2+}, Fe^{2+} and Fe^{3+}. Interestingly, as summarized in **Table S1**, the various reported sensors are quite specific, either for Cu^{2+} or Fe^{2+} or Fe^{3+} or for Cu^{2+} and Fe^{3+} or for Fe^{2+} and Fe^{3+} [4,5,21-28,30], but to the best of our knowledge, a colorimetric chemosensor for the simultaneous detection of Cu^{2+}, Fe^{2+} and Fe^{3+} ions remains unreported. Herein, as a part of our efforts in the field [29-33], the chemosensor **AM-1** has been developed for the selective and sensitive detection of Cu^{2+}, Fe^{2+} and Fe^{3+} ions in aqueous solution.

2. Results and Discussion

The receptor **AM-1** was efficiently synthesized by the reaction of 2-cyanopyridine and 4-bromoaniline in the presence of $TiCl_4$ (Scheme 1) [34]. The molecular structure of **AM-1** was established by FT-IR, MS, ^{1}H-NMR spectra and by elemental analyses [Figure S1-3]. The cation recognition ability of **AM-1** towards different metal ions was studied by experimental (naked-eye, UV-visible, and fluorescence methods) and theoretical methods.

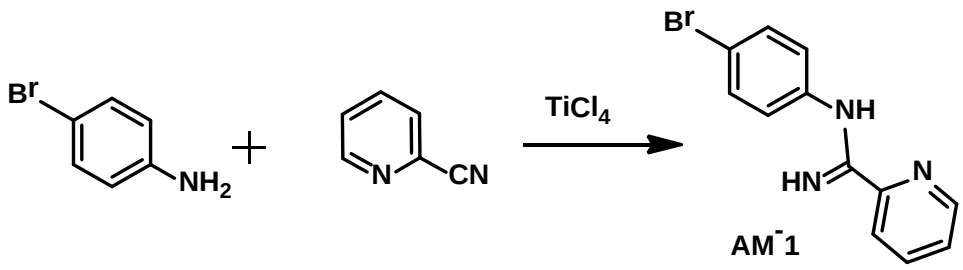

Scheme 1. Synthesis of receptor **AM-1.**

2.1. Colorimetric and UV-Vis study

The color and absorption spectra of the receptor **AM-1** (5 x 10^{-5} M, in methanol) was studied in the absence and presence of 5 equivalents of different metal ions such as Sr^{2+}, Cr^{3+}, Co^{2+}, Ni^{2+}, Zn^{2+}, Ag^{+}, Al^{3+}, Ba^{2+}, Ca^{2+}, Cd^{2+}, Hg^{2+}, K^{+}, Li^{+}, Mg^{2+}, Mn^{2+}, Na^{+}, Pb^{2+}, Cu^{2+}, Fe^{2+} and Fe^{3+} (1 x 10^{-2} M, in water). Receptor **AM-1** exhibited two absorption bands at 225 nm and 272 nm. Upon addition of Fe^{3+} ions to the solution of **AM-1**, significant spectral changes were observed (Figure 1). A hypochromic shift was observed at 225 nm while a blue shift of 6 nm was observed at 272 nm with the appearance of a new broad charge transfer band between 350-450 nm. The charge transfer band was also observed in the presence Cu^{2+} and Fe^{2+}, but the intensity was lower. The spectral changes associated with **AM-1** are presumably due to the delocalization of electrons from the imine nitrogen (C=N) of the amidine during complexation with the metal ions; an intermolecular charge transfer (ICT) can occur between the metal ions and the imine nitrogen of **AM-1**. However, no significant changes in the absorption spectrum of **AM-1** were observed with other metal ions, thereby revealing the selectivity toward Cu^{2+}, Fe^{2+} and Fe^{3+}.

The absorption titrations of **AM-1** with the metal ions (Cu^{2+}, Fe^{2+} and Fe^{3+}**)** were carried out to examine the recognition ability. As shown in Figure 2, on successive addition of incremental amounts of Fe^{3+} to the **AM-1** solution, the receptor bands were gradually shifted with the appearance of a new charge transfer band. Using the absorption titration data, the binding constant of 1.0 x 10^{5} M^{-1} was calculated from the Benesi-Hildebrand Plot (Figure

S4). The detection and quantification limits of 6.5 x 10^{-7} M and 1.9 x 10^{-6} M, respectively for Fe^{3+} were estimated (Figure S5). The binding constants calculated for the metal ions Cu^{2+} and Fe^{2+} were respectively 5.0 x 10^{3} M^{-1} and 9.7 x 10^{-1} M^{-1} from the Benesi-Hildebrand Plots (Figure S6-7), comparatively lower than found for Fe^{3+}.

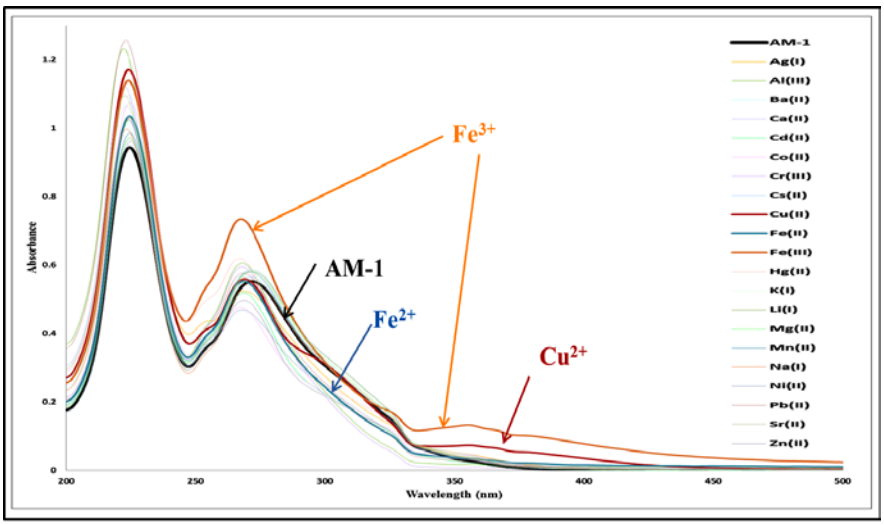

Figure 1. Absorbance spectral changes of **AM-1** (5 x 10^{-5} M, in methanol) upon addition of 5 equivalents of various metal ions (1 x 10^{-2} M, in water).

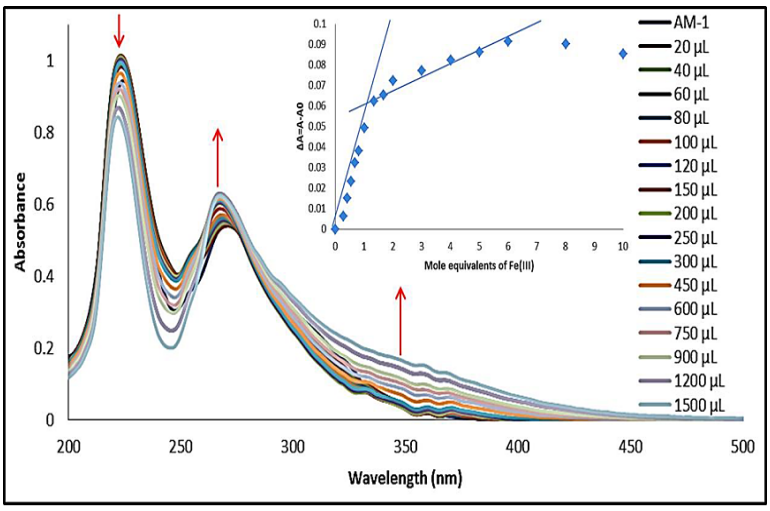

Figure 2. Absorption spectral changes of **AM-1** (5 x 10^{-5} M, in methanol) upon addition of 0 - 10 equivalents of Fe^{3+} (1 x 10^{-3} M, in water). Inset shows the mole ratio plot from absorption titration of **AM-1** with Fe^{3+}.

The stoichiometry of **AM-1**.Fe^{3+} was calculated through Job's plot (Figure 3), with the latter plotted between the mole fractions of Fe^{3+} and the absorption changes at 267 nm, where the maxima was obtained at a molar fraction of 0.5, which indicates the formation of a ferric complex in 1:1 stoichiometry. Further, stable **AM-1**.Fe^{2+} and **AM-1**.Cu^{2+} complexes were synthesized and characterized by LC-MS. The proposed 1:1 stoichiometry for both **AM-1**.Fe^{2+} and **AM-1**.Cu^{2+} complexes was supported by the obtained mass data (Figure S8-9).

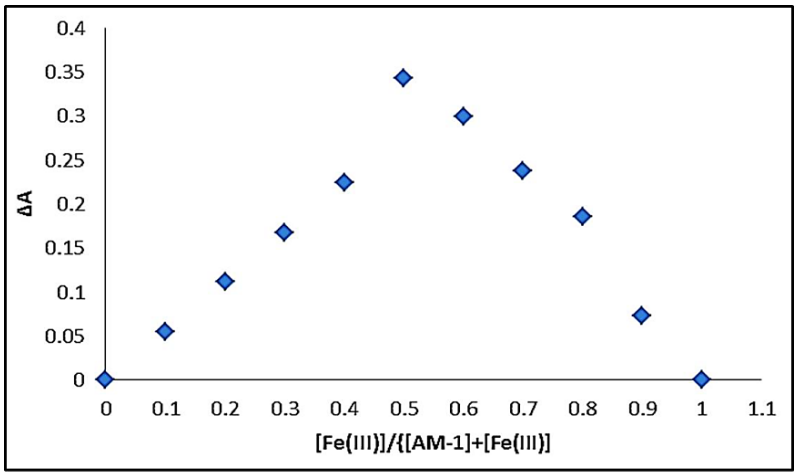

Figure 3. Jobs Plot for **AM-1** and Fe^{3+}, indicating the formation of a 1:1 (L:M) complex.

Significant colour changes of the **AM-1** solution were observed upon addition of Fe^{3+}, Fe^{2+} and Cu^{2+} over the other tested metal ions (Figure 4). A distinct colour change of **AM-1** from colourless to red, orange and green was observed in the presence of Fe^{2+}, Fe^{3+} and Cu^{2+} ions respectively, which indicated the sensitive and selective 'naked-eye' detecting ability for these cations. By utilizing the benefits of the 'naked-eye' results, we have applied receptor **AM-1** as an indicator for the '*in situ*' qualitative detection of Fe^{3+}, Fe^{2+} and Cu^{2+} (Figure 5). A solution of receptor **AM-1** (1 x 10^{-3} M, in methanol) is colourless. After addition of 1 equivalent of Fe^{2+}, it turns to dark blood red color. To this red color solution, addition of 0.1 M $K_2Cr_2O_7$ solution changes the colour from dark red to faint yellow, which supports the

conversion of Fe^{2+} into Fe^{3+}. On further addition of $NaBH_4$, the observed faint yellow colour reversibly converted into a dark red colour and with excess $NaBH_4$, the colour again changes to colourless. These results inferred that we can monitored the presence of both oxidation states of iron (Fe^{2+} and Fe^{3+}) by using the receptor **AM-1**. In another experiment, we have added copper powder to the colourless solution of receptor **AM-1**. To this colourless mixture, the addition of $AgNO_3$ solution resulted in a remarkable colour change from colorless to green, which supports the conversion of metallic copper into the Cu^{2+} state. It is very interesting to mention here that all three ions (Fe^{2+}, Fe^{2+} and Cu^{2+}) shows reversibility in the colour change on addition of aq. EDTA solution. The above obtained naked-eye results opens the door for applications of such chemosensor for the '*in situ*' qualitative determination of three ions, namely Fe^{3+}, Fe^{2+} and Cu^{2+}.

Figure 4. Photo of the vials containing **AM-1** (1 x 10^{-3} M, in methanol) in the presence of various metal ions (1 x 10^{-2} M, in water).

Figure 5. '*In situ*' qualitative detection of Fe^{3+}, Fe^{2+} and Cu^{2+}.

2.2. Fluorescence study

The cation binding behaviour of **AM-1** was also investigated by emission measurements. Addition of Fe^{3+} ions (5 equivalents) to the **AM-1** solution in methanol results in a distinct fluorescence quenching (Figure 6). However, in the presence of other metal ions such as Sr^{2+}, Cr^{3+}, Co^{2+}, Ni^{2+}, Zn^{2+}, Ag^{+}, Al^{3+}, Ba^{2+}, Ca^{2+}, Cd^{2+}, Hg^{2+}, K^{+}, Li^{+}, Mg^{2+}, Mn^{2+}, Na^{+} and Pb^{2+}, the fluorescence intensity of **AM-1** at 305 nm either did not induce any significant changes or was slightly enhanced under identical conditions.

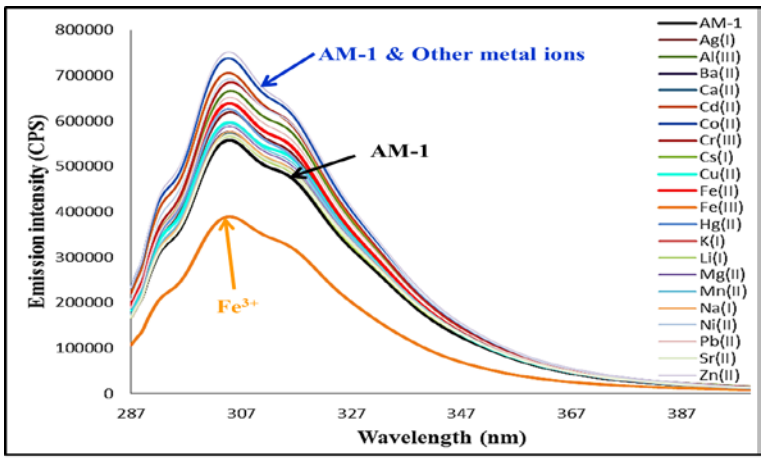

Figure 6. Fluorescence spectral (λ_{ex}= 277 nm) changes of **AM-1** (5 x 10^{-5} M, in methanol) upon addition of 5 equivalent of various metal ions (1 x 10^{-2} M, in water).

The fluorescence titration of **AM-1** (5 x 10^{-5} M, in methanol) with Fe^{3+} (1 x 10^{-3} M, in water) was performed via the successive addition of incremental concentrations of Fe^{3+}. The fluorescence intensity of **AM-1** was gradually quenched at 305 nm (Figure 7). In another experiment, the Fe^{3+} sensing ability of **AM-1** under a competition environment was investigated in the presence of potentially interfering metal ions by fluorescence measurements (Figure S10). For methanol solutions of **AM-1**, addition of 2 equiv. of Fe^{3+} in the presence of 2 equiv. of other tested metal ions caused a dramatic quenching in the fluorescence intensity of **AM-1** with either very slight or no interference effects. Therefore, it

was concluded that **AM-1** is a reliable, highly selective and sensitive turn-off fluorescent sensor for Fe^{3+}. Based on the fluorescence titration data, the detection and quantification limits of 1.4 x10^{-5} M and 4.1 x 10^{-5} M respectively for Fe^{3+} were estimated (Figure S11). Also, the binding constant (*K*) of **AM-1** with Fe^{3+} was determined by a Benesi-Hildebrand plot (Figure S12) and a Scatchard plot (Figure S13) from the fluorescence titration data. The binding affinity of **AM-1** was found to be ≈ 1 x 10^5 M^{-1} for Fe^{3+}.

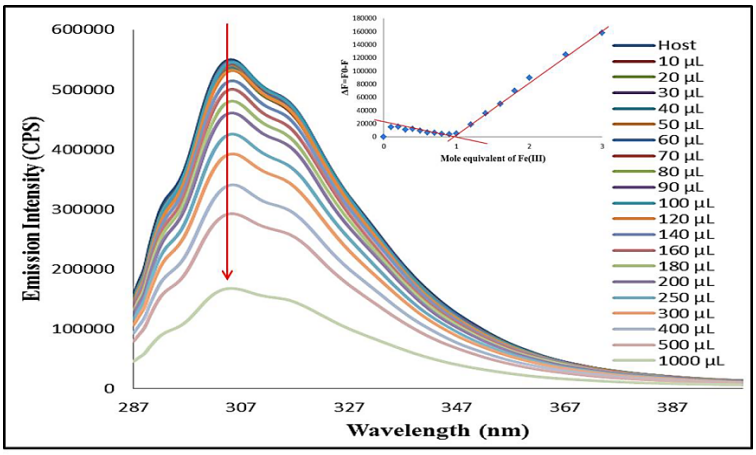

Figure 7. Fluorescence spectral changes of sensor **AM-1** (5 x 10^{-5} M, in methanol) upon addition of 0 - 10 equivalents of Fe^{3+} (1 x 10^{-3} M, in water) at λ_{ex}=277 nm. Inset showing the mole ratio plot from fluorescence titration of **AM-1** with Fe^{3+}.

The quenching can be mathematically expressed by the Stern–Volmer Eq. (1), which allows us to determine the type of quenching. If the Stern Volmer plot is linear then the quenching is of a static type rather than dynamic quenching. For the **AM-1**.Fe^{3+} ions, the linear Stern Volmer plot indicates that static quenching is obtained [35]. This confirmed the formation of only one type of complex between the receptor **AM-1** and the Fe^{3+} ions.

$$F_0/F = 1 + k_q\tau_0[Q= 1 + K_{sv}[Q] \qquad (1)$$

Where F_0 and F are the fluorescence intensities in the absence and presence of the quencher, $k_q$is the bimolecular quenching constant, τ_0 is the lifetime of the fluorescence in the absence of the quencher [Q] is the concentration of the quencher, and K_{sv} is the Stern–

Volmer quenching constant. In the presence of a quencher, the fluorescence intensity is reduced from F_0 to F. The ratio (F_0/F) is directly proportional to the quencher concentration [Q]. Evidently:

$$K_{sv} = k_q \qquad (2)$$

$$F_0/F = 1 + K_{sv}\,[Q] \qquad (3)$$

According to Eq. (3), a plot of F_0/F *versus* [Q] shows a linear graph with an intercept of **AM-1** and a slope of K_{sv}. A typical plot of F_0/F *versus* Fe^{3+} concentration is shown in Figure 8.

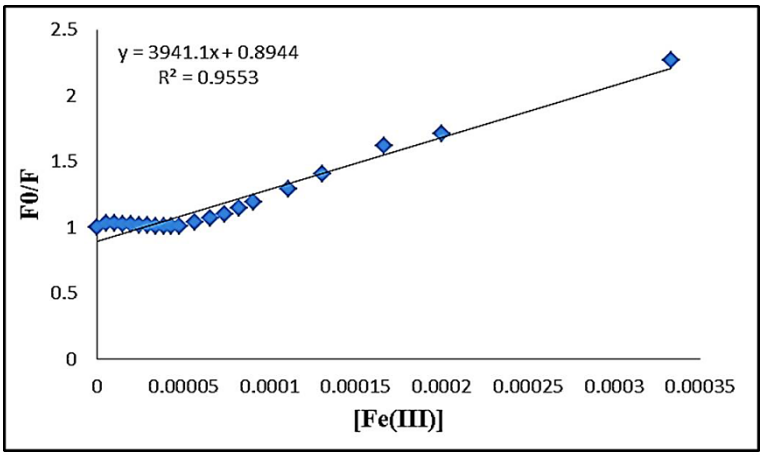

Figure 8. Stern-Volmer Quenching Plot for $Fe^{3+}$with receptor **AM-1**.

2.3. Computational study

In the absence of a suitable single crystal of **AM-1** and its complexes, and to get more insight into the above experimental observations, DFT calculations were performed to understand the electronic environment and the changes in the structure of **AM-1** upon complexation with Fe^{3+}, Fe^{2+} and Cu^{2+}. During the computational study, two stable conformations of **AM-1** (L and L') were optimized (Figure 9). The form L is relatively more stable than L' by 5.01 kcal/mol. There is an intramolecular H-bond (2.036 Å) between the amine proton (H6) with the pyridine-N atom. The ligand exhibited two possible coordination modes (Figure 10, mode I: Py-N and =NH and mode II: Py-N and –NH) forming a five membered chelate ring with the metal ions. According to the calculated relative energy, the

complexes preferred to coordinate through the Py-N and =NH. The Cu^{2+}, Fe^{2+} and Fe^{3+} complexes with the coordination mode I is relatively more stable than mode II by 25.15 kcal/mol, 7.36 kcal/mol and 54.32 kcal/mol, respectively. The interaction energy was calculated by applying the equation [E_{int} = E (ML)–E(L)-E(M)]. The E_{int} for the **AM-1.**Fe^{3+}, **AM-1.**Fe^{2+} and **AM-1.**Cu^{2+} complexes are -792.58 kcal/mol, -286.83 kcal/mol and -330.29 kcal/mol, respectively. This result indicates that Fe^{3+} is forming a stronger complex with **AM-1** followed by Cu^{2+} and then Fe^{2+}.

The plots of the frontier molecular orbitals of **AM-1** and its complexes with Fe^{3+}, Cu^{2+} and Fe^{2+} were analysed. As shown in Figure S14 and S15, the electron density of the HOMO and LUMO of the receptor located in two different rings suggests a strong intramolecular charge transfer. On complexation, the lowering of the band gap indicates a blue-shift in the absorption band, and simultaneously the HOMO and LUMO indicates the formation of a charge-transfer complex between the receptor and metal ions.

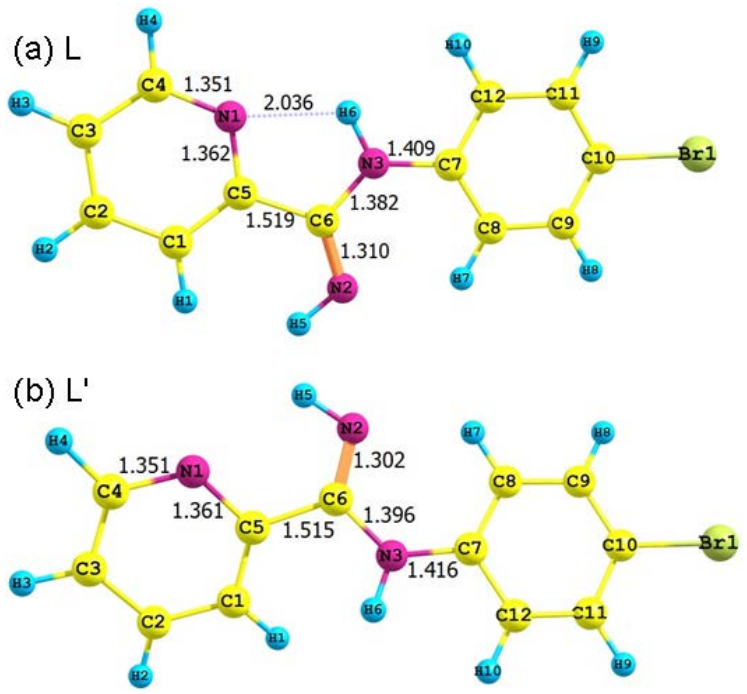

Figure 9. Optimized structure of the two probable conformations (**L** and **L'**) of **AM-1** at B3LYP/SDD method.

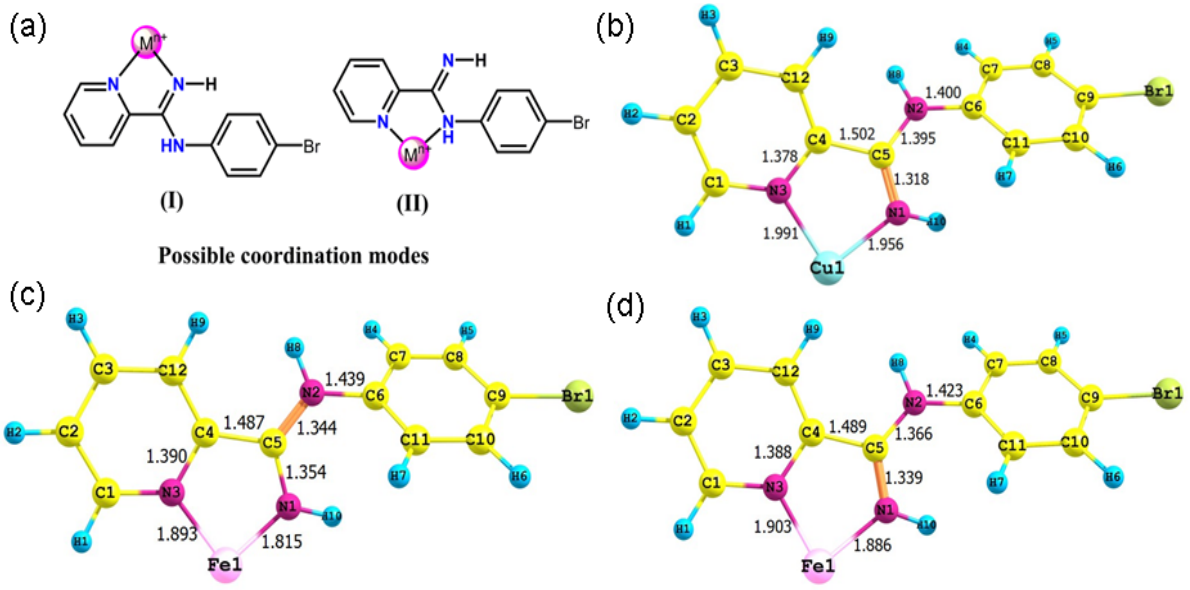

Figure 10. (a) The possible coordination modes of **AM-1**, and the favourable optimized structure of the complexes (b) **AM-1.**Cu^{2+}, (c) **AM-1.**Fe^{2+} and (d) **AM-1.**Fe^{3+} at B3LYP/SDD method.

3. Materials, Methods and Instrumentations

All the starting reagents and metal perchlorates were purchased either from S. D. Fine chemicals or Sigma Aldrich depending on their availability. All the reagents were used as received. All the solvents were of spectroscopic grade and were used without further treatment. The purity of the compounds and the progress of the reactions were determined and monitored by means of analytical thin layer chromatography (TLC). Pre-coated silica gel 60 F254 (Merck) on alumina plates (7 X 3 cm) were used and visualized by using either an iodine chamber or a short UV-Visible lamp. Melting points were recorded on the Celsius scale by open capillary method and are uncorrected. IR spectra were recorded on a Perkin-Elmer Spectrum One FT-IR spectrometer as potassium bromide pellets and nujol mulls, unless otherwise mentioned. IR bands are expressed in frequency (cm^{-1}). NMR spectra were recorded in $CDCl_3$ on a Varian (Mercury Vx) SWBB Multinuclear probe spectrometer, operating at 300 MHz and 75 MHz for ^{1}H NMR and ^{13}C NMR, respectively and shifts are given in ppm downfield from TMS as an internal standard. UV-Vis spectra were recorded on

a U-3900 spectrophotometer (Perkine Elmer Co., USA) with a quartz cuvette (path length = 1 cm). Fluorescence spectra were recorded on a Fluoromax-4 spectrofluorometer (HORIBA Jobin Yvon Co., France).

3.1. Synthesis of AM-1

In 250 ml dry round bottom flask, a mixture of 4-bromoaniline (1.28 g, 10 mmol) and 2-cyanopyridine (1.04 g, 10 mmol) was heated after fitting of dry condenser along with a guard tube, in an oil bath, at a temperature range of 110-120 ^{0}C with constant stirring. After 30 min., $TiCl_4$ (1.33 ml, 12 mmol) was added to the flask. After addition, the temperature was increased to 150-160 ^{0}C, and heating continued for 3-4 h. The reaction progress was monitored by TLC. After completion of the reaction, the obtained solid was cooled to room temperature and then was dissolved in hot water and made alkaline with 10 % NaOH solution. This alkaline solution was extracted with dichloromethane [3 x 50 mL]. The organic layer was decolorized with activated charcoal and dried over anhydrous Na_2SO_4. After evaporating the solvent under reduced pressure, the crude amidine was obtained. This crude amidine was recrystallized from a acetone:hexane [10:90] system, to afford pure amidine. Yield: 2.24 g (81 %).

IR [KBr, cm^{-1}]: 3376, 2854, 1640, 1577, 1530, 1459, 1377, 1321, 1300, 1260, 1151, 1119, 1096, 1006, 818, 769, 722, 541. **LCMS [ESI, e/z (%)] :** 278 (100), 276 (100), 260 (20), 259 (20). **^{1}H NMR [$CDCl_3$, 300 MHz]:** 5.85 (br s, 2H, NH, C=NH), 6.88-6.91 (d, J=8.7 Hz, 2H, ArH), 7.38-7.50 (m, 3H, ArH), 7.79-7.84 (m, 1H, ArH), 8.36-8.39 (d, J=8.1Hz, 1H, ArH), 8.56-8.58 (m, 1H, ArH). Anal.calcd for $C_{12}H_{10}BrN_3$: C, 52.20; H, 3.65; N, 15.22. Found: C, 52.54; H, 3.60; N, 15.28.

3.2. Spectroscopic Study

Stock solutions of the sensor **AM-1** (1.0 ×10^{-3} M) and cations (1.0 ×10^{-2} M) were prepared in methanol and water, respectively. These solutions were used for all spectroscopic

studies after appropriate dilution. For spectroscopic titrations, the required amount of the diluted receptor **AM-1** was taken directly into a cuvette and the spectra were recorded after successive addition of the cations by using a micropipette.

3.3. Computational analysis

The structural optimization of the ligand and its complexes with the metal ions (Cu^{2+}, Fe^{2+} and Fe^{3+}) has been performed in the gas phase using the computer program Gaussian 09W [36] by applying the Density functional theory (DFT) method. DFT calculations were performed with a hybrid functional B3LYP (Becke's three parameter hybrid functional using the LYP correlation functional) using the basis sets SDD. Then, the optimized geometries have been confirmed by frequency analyses at the same level of theory to ascertain the optimized structure were stable.

4. Conclusion

In summary, we have prepared an easy-to-make amidine based receptor **AM-1** for the selective detection of Fe^{2+}, Fe^{3+} and Cu^{2+} ions as evidenced by colour change and UV-Vis spectra. The 1:1 stoichiometry for the **AM-1**.Fe^{3+}, **AM-1**.Fe^{2+}, and **AM-1**.Cu^{2+} complexes was proposed by Job's plot and LC-MS analysis. Additionally, the receptor exhibited a highly selective and sensitive fluoresce turn-off response in the presence of Fe^{3+}. The detection and quantification limits for receptor **AM-1** for Fe^{3+} were estimated at 6.5×10^{-7} M and 1.9×10^{-6} M, respectively from absorption measurements, whereas values of 1.4×10^{-5} M and 4.1×10^{-5} M, respectively were obtained from emission measurements. The receptor **AM-1** with its' low cost, ease of preparation, and impressive selectivity, suggests that this approach could potentially lead to many more sensors being designed using the amidine moiety as a core skeleton.

5. Acknowledgement

The author Dr. U. D. Patil is grateful to Department of Science & Technology, New Delhi, INDIA (Reg. No. CS-088/2013) and 'North Maharashtra University, Jalgaon', VCRMS Scheme, for the financial support.

Appendix A. Supplementary data

†Electronic Supplementary Information (ESI) available: See DOI: 10.1039/c000000x/

6. References - these are in ACS format!

[1] Bell TW, Hext NM. Supramolecular optical chemosensors for organic analytes. Chem Soc Rev 2004; 33: 589-8.

[2] Suksai C, Tuntulani T. Luminescent Chemodosimeters for Bioimaging. Chem Soc Rev 2003; 32: 192-2.

[3] Kuan Z, Yue LC, Ping HL, Fang L. Chromo-chemodosimetric detection for Fe^{2+} by Fenton reagent-induced chromophore-decolorizing of halogenated phenol sulfonphthalein derivatives. Science China Chemistry 2010; 53: 1398-5.

[4] Liang ZQ, Wang CX, Yang JX, Gao HW, Tian YP, Tao XT, Jiang MH. A highly selective colorimetric chemosensor for detecting the respective amounts of Iron(II) and Iron(III) ions in water. New J Chem 2007; 31: 906-0.

[5] Sen S, Sarkar S, Chattopadhyay B, Moirangthem A, Basu A, Dharad K, Chattopadhyay P. A ratiometric fluorescent chemosensor for iron: discrimination of Fe^{2+} and Fe^{3+} and living cell application. Analyst 2012; 137: 3335-2.

[6] Bhalla V, Arora H, Kumar M. Aggregates of a triphenylene based chemosensing ensemble for sensitive detection of cyanide ions in an aqueous medium. Dalton Trans 2013; 42: 4450-5.

[7] Silva AP, Gunaratne HQN, Gunnlaugsson T, Huxley AJM, McCoy CP, Rademacher JT, Rice TE. Signaling recognition events with fluorescent sensors and switches. Chem Rev 1997; 97: 1515-6.

[8] Valeur B, Leray I. Design principles of fluorescent molecular sensors for cation recognition. Coord Chem Rev 2000; 205: 3-0.

[9] Silva AP, McCaughan B, McKinney BOF, Querol M. Newer optical-based molecular devices from older coordination Chemistry. Dalton Trans 2003; 1902-3.

[10] Callan JF, Silva AP, Magri DC. Luminescent sensors and switches in the early 21st century. Tetrahedron 2005; 61: 8551-8.

[11] Sahoo SK, Sharma D, Bera RK, Crisponi G, Callan JF. Iron(III) selective molecular and supramolecular fluorescent probes. Chem Soc Rev 2012; 41: 7195-7.

[12] Crabtree RH. Metal Ions at Work. Science 1994; 266: 1591-2.

[13] Burdo JR, Connor JR. Brain iron uptake and homeostatic mechanisms: an overview. BioMetals 2003; 16: 63-5.

[14] Pithadia AS, Lee MH. Metal-associated amyloid-β species in Alzheimer's disease. Curr Opin Chem Biol 2012; 16: 67-3.

[15] High B, Bruce D, Richter MM. Determining copper ions in water using electrochemilumincenec. Anal Chim Acta 2001; 449: 17-2.

[16] Zhang LZ, Wang LY, Fan JL, Guo KX, Peng XJ. A highly selective, fluorescent chemosensor for bioimaging of Fe^{3+}. Bioorg Med Chem Lett 2011; 21; 5413-6.

[17] Brewer GJ. Overview of the role of copper in neurodegenerative diseases and potential treatment with tetrathiomolybdate. Cell Biol Toxicol 2008; 24: 423-6.

[18] Barnham KJ, Bush AI. Metals in Alzheimer's and Parkinson's diseases. Curr Opin Chem Biol 2008; 12: 222-8.

[19] Li ZX, Zhang LF, Wang LN, Guo YK, Cai LH, Yu MM, Wei LH. Highly sensitive and selective fluorescent sensor for Zn^{2+}/Cu^{2+} and new approach for sensing Cu^{2+} by central metal displacement. Chem Commun 2011; 47: 5798-0.

[20] Jeong YS, Yoon JY. Recent progress on fluorescent chemosensors for metal ions. Inorg Chim Acta 2012; 381: 2-4.

[21] Shellaiah M, Wu YH, Singh A, Raju MVR, Lin HC. Novel pyrene- and anthracene-based Schiff base derivatives as Cu^{2+} and Fe^{3+} fluorescence turn-on sensors and for aggregation induced emissions. J Mater Chem A 2013; 1: 1310-8.

[22] Li J, Hu Q, Yu X, Zeng Y, Cao C, Liu X, Guo J, Pan Z. A novel rhodamine-benzimidazole conjugate as a highly selective turn-on fluorescent probe for Fe^{3+}. J Fluoresc 2011; 21: 2005-3.

[23] Hu ZQ, Wang XM, Feng YC, Ding L, Li M, Lin CS. A novel colorimetric and fluorescent chemosensor for acetate ions in aqueous media based on a rhodamine 6G–phenylurea conjugate in the presence of Fe(III) ions. Chem Commun 2011; 47: 1622-4.

[24] Yang Z, Yan C, Chen Y, Zhu C, Zhang C, Dong X, Yang W, Guo Z, Lu Y, He W. A novel terpyridine/benzofurazan hybrid fluorophore: metal sensing behavior and application. Dalton Trans 2011; 40: 2173-6.

[25] Pathak RK, Hinge VK, Mondala P, Rao CP. Ratiometric fluorescence off-on-off sensor for Cu^{2+} in aqueous buffer by a lower rim triazole linked benzimidazole conjugate of calix[4]arene. Dalton Trans 2012; 41: 10652-0.

[26] Singh N, Mulrooney RC, Kaur N, Callan JF. A nanoparticle based chromogenic chemosensor for the simultaneous detection of multiple analytes Chem Commun 2008; 4900-2.

[27] Jiang Z, Tang L, Shao F, Zheng G, Lu P. Synthesis and characterization of 9-(cycloheptatrienylidene)fluorene derivatives : New fluorescent chemosensors for detection of Fe^{3+} and Cu^{2+}. Sensors and Actuators B 2008; 134: 414-8.

[28] Zhao XJ, He RX, Li M, Zhao NW, Li YF, Huang CZ. Formation of blue fluorescent ribbons of 4',4""-(1,4-phenylene)bis(2',:6',2''-terpyridine) and highly selective visual detection of iron(II) cations. RSC Adv 2013; 3: 111-6.

[29] Tayade KC, Kuwar AS, Fegade UA, Sharma H, Singh N, Patil UD, Attarde SB. Design and synthesis of a pyridine based chemosensor : highly selective fluorescent probe for Pb^{2+}. J Fluoresc 2013; DOI 10.1007/s10895-013-1287-6.

[30] Kuwar AS, Fegade UA, Tayade KC, Patil UD, Puschmann H, Gite VV, Dalal DS, Bendre RS. Bis(2-hydroxy-3-isopropyl-6-methyl-benzaldehyde)ethylenediamine: A novel cation sensor. J Fluoresc 2013; 23: 859-4.

[31] Patil R, Moirangthem A, Butcher R, Singh N, Basu A, Tayade KC, Fegade UA, Hundiwale DH, Kuwar AS. Al^{3+} selective colorimetric and fluorescent red shifting chemosensor : Application in living cell imaging. Dalton Trans 2013; DOI: 10.1039/b000000x.

[32] Tayade KC, Gallucci J, Sharma H, Attarde SB, Patil R, Singh N, Kuwar AS. Exploration of selective recognition of iodide with dipodal sensor: 2,2'-[ethane-1,2-diylbis(iminoethane-1,1-diyl)] diphenol. Dalton Trans 2013; DOI: 10.1039/b000000x.

[33] Sharma D, Sahoo SK, Chaudhary S, Bera RK, Callan JF. Fluorescence 'turn-on' sensor for F^{-} derived from vitamin B6 cofactor. Analyst 2013; 138: 3646-0.

[34] Patil UD, Mahulikar PP. A convenient, $TiCl_4$ / $SnCl_4$ mediated synthesis of *N*-phenyl or *N*-aryl benzamidines and *N*-phenylpicolinamidines. ISRN Organic Chemistry 2012; Article ID 963195, 1-6; doi:10.5402/2012/963195.

[35] Stern O, Volmer M. Uber die abklingungszeit der fluoreszenz. Phys J 1919; 20: 183-8.

[36] Schlegel HB, Scuseria GE, Robb MA, Cheeseman JR, Scalmani G, Barone V, Mennucci B, Petersson GA, Nakatsuji H, Caricato M, Li X, Hratchian HP, Izmaylov AF, Bloino J, Zheng G, Sonnenberg GJ, Hada M, Ehara M, Toyota K, Fukuda R, Hasegawa J, Ishida M, Nakajima T, Honda Y, Kitao O, Nakai H, Vreven T, Montgomery JA, Peralta JE, Ogliaro F, Bearpark M, Heyd JJ, Brothers E, Kudin KN, Staroverov VN, Kobayashi R, Normand J, Raghavachari K, Rendell A, Burant JC, Iyengar SS, Tomasi J, Cossi M, Rega N, Millam JM, Klene M, Knox JE, Cross JB, Bakken V, Adamo C, Jaramillo J, Gomperts R, Stratmann RE, Yazyev O, Austin AJ, Cammi R, Pomelli C, Ochterski JW, Martin RL, Morokuma K, Zakrzewski VG, Voth GA, Salvador P, Dannenberg JJ, Dapprich S, Daniels AD, Farkas Ö, Foresman JB, Ortiz JV, Cioslowski J, Fox DJ. Gaussian 09, Revision A.1, Gaussian, Inc., Wallingford CT, 2009.